

Water-Soluble Py-BIPS Spiroyrans as Photoswitches for Biological Applications

Cem Özçoban,^{||,†} Thomas Halbritter,^{||,†} Sabrina Steinwand,^{||,‡} Lisa-Marie Herzig,[‡] Jörg Kohl-Landgraf,[‡] Noushin Askari,[†] Florian Groher,[§] Boris Fürtig,[†] Christian Richter,[†] Harald Schwalbe,[†] Beatrix Suess,[§] Josef Wachtveitl,^{*,‡} and Alexander Heckel^{*,†}

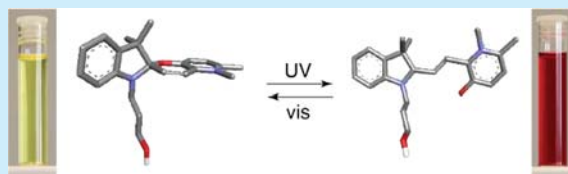
[†]Goethe-University Frankfurt, Institute for Organic Chemistry and Chemical Biology, Max-von-Laue-Str. 9, 60438 Frankfurt (M), Germany

[‡]Goethe-University Frankfurt, Institute for Physical and Theoretical Chemistry, Max-von-Laue-Str. 7, 60438 Frankfurt (M), Germany

[§]Technical University of Darmstadt, Department of Biology, Schnittspahnstr. 10, 64287 Darmstadt, Germany

S Supporting Information

ABSTRACT: The ultrafast photochemistry of a new spiropyran photoswitch (Py-BIPS) has been investigated, revealing many advantages in the application in water over the previously studied spiroyrans. Functionalized Py-BIPS derivatives are presented for the study of pH dependence, stability, toxicity, and the thermal and photochemical behavior on longer time scales in aqueous media using several spectroscopic methods. These investigations pave the way for the practical use of Py-BIPS derivatives as photoswitchable ligands of biomolecules.



Photochromic molecules can exist in different photoisomeric forms; they allow a variety of fascinating applications ranging from data storage, temperature measurements, and functionalization of nanodevices to the regulation of biological processes.^{1–4} Trauner and Sigel for example have shown that azo-propofols can perform light-dependent anesthesia in tadpoles.⁵ Tanaka and Asanuma used azobenzene-modified DNA to open DNA nanocontainers, and Liang and Asanuma induced a seesaw-like movement in DNA architectures.^{6,7} Koçer and Feringa opened and closed a channel protein with light using spiroyrans.⁸

While numerous applications of photochromic molecules have been reported in material sciences, their application in biology has remained challenging. The photochromic molecule often contains aromatic moieties that lead to poor solubility in aqueous media. Hydrolysis or side reactions in a cellular environment can result in loss of photochromic behavior. Many azobenzenes, for example, are known to be reduced by glutathione.⁹ In addition, both photochromic forms should provide distinct spectral absorption properties to facilitate a selective addressability. For a good photoswitching effect the two photoisomers should be as different in geometry and/or polarity or other properties as possible. Also the quantum yields and the respective switching amplitudes should be sufficiently high so that either form can accumulate in a fast and quantitative manner. Besides the influence of the cellular environment on the photoswitch, also the photoswitch itself should have a low toxicity and must not induce unwanted side reactions with the environment.

Spiroyrans are photochromic molecules that can be switched between a closed spiropyran (SP) form and an open merocyanine (MC) form (Figure 1). They represent an

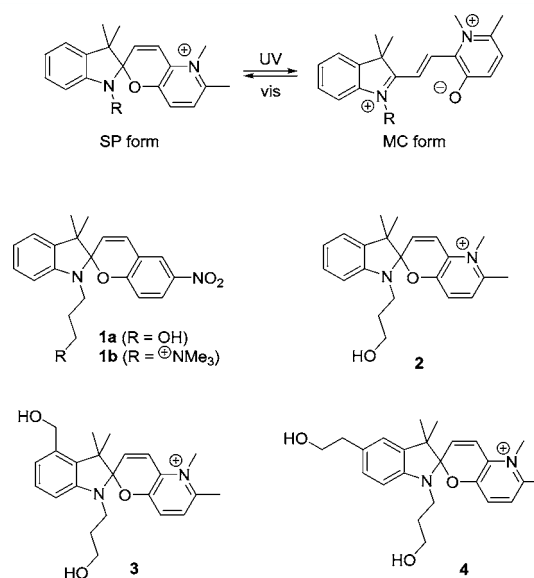


Figure 1. Overview of spiroyrans. Compounds 2–4 are studied in this investigation. Compounds 1a/b are shown for reference purposes. Each of these compounds can exist in the closed, yellowish spiropyran (SP) form or the open, red merocyanine (MC) form.

interesting alternative to azobenzene or diarylethene¹⁰ photoswitches. The pH-dependent behavior as well as the interaction of spiroyrans with DNA and with liposomes has been studied by

Received: February 6, 2015

Published: March 11, 2015

Andréasson et al.^{11–13} In spiropyrans the two photoisomers differ significantly in their geometry and dipole moment. The SP form has two perpendicular planes while the MC form is rather flat and has a higher polarity.¹⁴ However, the application of spiropyrans in biological contexts has been disappointing in a number of studies due to reported hydrolysis of the MC form in a retro-aldol reaction after addition of water¹⁵ and due to a loss of photoswitchability after conjugation to oligonucleotides.^{16,17} These findings were obtained for derivatives of Nitro-BIPS (**1a**) which was used as the progenitor spiropyran in a number of studies for a long time.

Recently, we introduced and characterized a different spiropyran (Py-BIPS, **2**) with superior properties in aqueous solution¹⁸ including retention of its photoswitching capability after covalent introduction into DNA.¹⁷ We suggested that this is due to the fact that Py-BIPS derivatives do not involve triplet states in the photochemical opening reaction, in contrast to Nitro-BIPS derivatives. While the previous study¹⁸ focused on the characterization of the ultrafast dynamics of the photo-reaction of Py-BIPS, the present study includes new derivatives of Py-BIPS and focuses on the pH dependence, stability, toxicity, and the thermal and photochemical behavior on longer time scales, employing optical and NMR spectroscopic techniques.

We have synthesized two additional derivatives of Py-BIPS (**3**, **4**) which bear a second hydroxyalkyl substituent that can be used for example for a two-point fixation of the spiropyran in a photoswitching scenario for example in DNA or in peptides. For the description of the synthesis we refer to the Supporting Information. All Py-BIPS derivatives of this study show excellent solubility in the millimolar range in aqueous buffers (28 mM in PBS pH 7.4 for **2**, 18 mM for **3**, and 77 mM for **4**) which is in contrast to a solubility of <0.05 mM for Nitro-BIPS (**1a**). Only the derivative **1b** of Andréasson has a similar water solubility of 57 mM in PBS pH 7.4.

Figure 2 gives an overview of the pure spectra (obtained by HPLC analysis) of the respective SP and MC forms. The

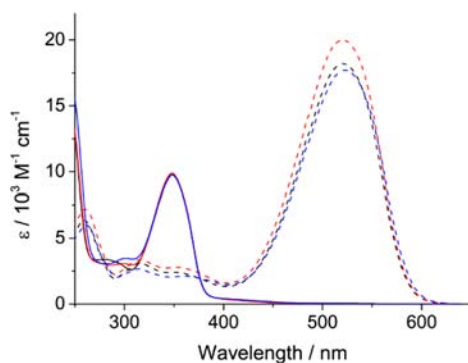


Figure 2. Spectra of the pure SP and MC forms of the compounds **2–4** obtained by HPLC analysis. It was confirmed that the amount of acetonitrile during the elution did not result in significant spectral changes (**2**, black curves; **3**, red curves; **4**, blue curves; SP, solid lines; MC, dashed lines).

maximum of the SP absorbance appears around 350 nm, whereas no other characteristic absorbance can be observed within the investigated spectral range. In contrast, the MC form shows a dominant absorbance around 520 nm. Hence both forms fulfill the mentioned criterion of distinct absorbances of both photoisomers very well. Importantly, at a wavelength of 350 nm a significant penetration depth can still be achieved in

skin tissue while other Nitro-BIPS derivatives are for example best irradiated at 254 nm for the ring-opening reaction which can be problematic for a biological application.¹³ The extinction coefficients appear to be in the same range for all three of our Py-BIPS derivatives. For the SP form, we determine $\epsilon \approx 9800 \text{ L} \cdot (\text{mol cm}^{-1})^{-1}$ at $\lambda_{\text{max}} = 350 \text{ nm}$. For the MC form we find $\epsilon \approx 19000 \text{ L} \cdot (\text{mol cm}^{-1})^{-1}$ at $\lambda_{\text{max}} = 520 \text{ nm}$ (for further details see Supporting Information).

Figure 3 shows an exemplary train of 10 photoswitching cycles of compound **4** in PBS (pH 7.4) with irradiation at 365 and

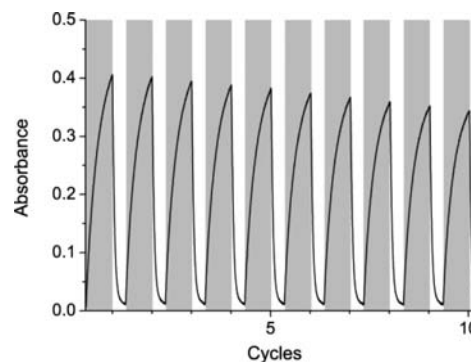


Figure 3. Absorbance change of compound **4** (0.1 mM) at 530 nm upon alternating irradiation with UV (365 nm, 50 mW, 3 min, gray areas) and visible light (530 nm, 100 mW, 1.5 min, white areas).

530 nm (the results obtained with the other compounds can be found in the Supporting Information). The first peak corresponds to a conversion to 23% of the MC form while under continued irradiation a maximum of 32% merocyanine was obtained. It can be seen that the switching behavior is very stable with only very little photofatigue. In comparison the Nitro-BIPS derivative **1b** of Andréasson showed even less photofatigue.¹³

For biological applications of spiropyrans a quantitative accumulation of one form is advantageous after being exposed to irradiation. The switching amplitude is mainly influenced by three factors: the absorbed light intensity, the quantum yield of the photochemical reactions, and the rate of the thermal back reaction which is opposed to the photochemical switching direction. The higher the absorbed light dose and quantum yield and the higher the energy barrier of the back conversion process, the higher the switching amplitude. With visible light around 530 nm for compounds **2–4** close to 100% SP form can be accumulated.

To investigate this we determined both the thermal conversion rates and the quantum yields of the photoreaction. The results are found in Table 1. The quantum yields for the photochemical opening reactions are comparable to the ones obtained with water-soluble Nitro-BIPS derivatives such as **1b** whereas the quantum yield for the photochemical closing reaction is about two times higher in our case.¹³ The rate of the thermal opening reaction k_{O} of **2** is 36 times slower than the one measured for **1b**, while the rate of the thermal closing reaction is 280 times faster.¹³ Hence in the case of Py-BIPS and its derivatives the thermal equilibrium is significantly shifted to the side of the SP form ($k_{\text{C}}/k_{\text{O}} \approx 15000$ compared to 1.44 for **1b**¹³), while the rate of the thermal closing reaction is still very low so that the MC form can be considered thermally stable in a reasonable experimental window. The Arrhenius graphs for the determination of the activation energy can be found in the Supporting Information.

Table 1. Comparison of Thermal and Photochemical Data of Compounds 2–4^a

	k_O ($10^{-6}\cdot\text{s}^{-1}$)	k_C ($10^{-2}\cdot\text{s}^{-1}$)	$E_{A,O}$ (kJ/mol)	$E_{A,C}$ (kJ/mol)	Φ_O (%)	Φ_C (%)
2	1.7 ± 0.2	2.4 ± 0.3	115 ± 2	71 ± 4	1.6 ± 0.1	10.0 ± 0.6
3	2.4 ± 0.3	3.7 ± 0.4	107 ± 2	63 ± 3	4.4 ± 0.2	13.3 ± 0.9
4	6.0 ± 0.6	2.8 ± 0.3	111 ± 4	77 ± 5	4.4 ± 0.2	9.2 ± 0.7

^aThermal rates (k) at 25 °C (extrapolated from Arrhenius graphs; see the Supporting Information), corresponding activation energies (E_A), and quantum yields (Φ) for opening (O) and closing (C) reaction, respectively.

We further investigated the pH dependence of the merocyanine population in thermal equilibrium. The results of the titration experiments can be found in Figure 4, and the pK_a

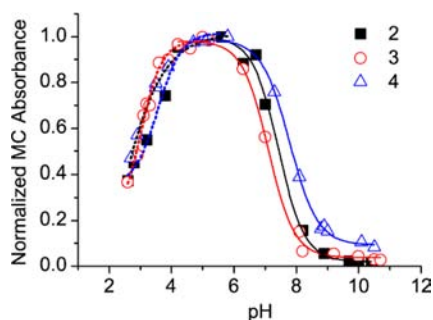


Figure 4. Results of pH titration studies with compounds 2–4. The absorbance was measured at 520 nm.

Table 2. Measured and Calculated pK_a /pH Values Derived from Figure 4

compd	$pK_a^{(1)}$ (exptl)	$pK_a^{(1)}$ (theor.)	$pH^{(2)}$ (exptl)
2	3.5	2.8	7.4
3	3.0	2.8	7.1
4	2.9	2.8	7.8

values are summarized in Table 2. In all compounds at a pH of around 3, the MC band disappears in the spectrum indicating that the phenolate of the molecule is protonated. The observed values ($pK_a^{(1)}$) are in good agreement with predictions¹⁹ and are about one unit on the pK_a scale more acidic than other water-soluble Nitro-BIPS derivatives such as for example **1b**.¹³

To interpret this pH-dependent behavior we performed NMR studies for compound 4 at pH 2.7, 6.9, and 10.0 with and without irradiation (Figures 5, 6 and Supporting Information). It is evident that in the thermal equilibrium at $T = 275$ and 298 K we could only detect the SP form irrespective of pH. Importantly, we did not observe any evidence for the existence of a tricyclic state with an *N,O*-ketal between the indolene part and the hydroxypropyl substituent. The determined coupling constant $^3J(\text{H}22,\text{H}23) = 11.7$ Hz for the double bond always indicates the expected (Z) configuration (for nomenclature, see Supporting Information). The signals of the two methyl groups of the indolene ring (H17, H18) as well as of the two proximal methylene groups (H13) of the hydroxypropyl substituent appear as two broad signals at pH 6.9 and 10.0 but as one distinct signal at pH 2.7. We explain these different line widths of the diastereotopic methyl and methylene groups by a fast thermal equilibration of the two enantiomeric forms of the spirocyanine where the *N,O*-ketal reversibly opens and closes after rotation of the chromene part. From ROESY and NOESY experiments, we determine the rate of conversion to be around 27 ± 5 s⁻¹ at

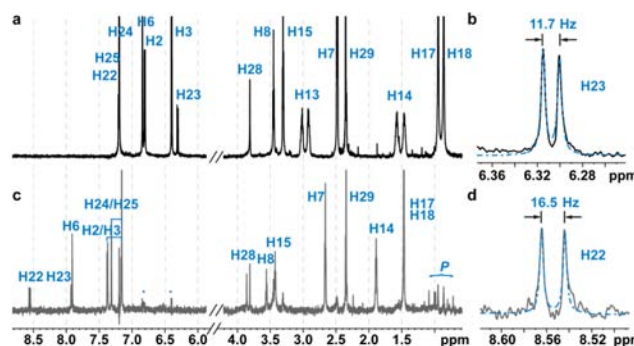


Figure 5. NMR spectra of SP and MC form of compound 4 at pH 6.9; (a) 1D ¹H NMR spectrum of SP; (c) 1D ¹H NMR spectrum of MC, difference spectrum of UV-irradiated sample minus spectrum of nonirradiated sample. The panels (b) and (d) display the change in $^3J(\text{H}22,\text{H}23)$ from 11.7 Hz in SP form to 16.5 Hz in MC form ($T = 275$ K). *: artifacts due to the formation of difference spectra; P: signals arising from photodegradation.

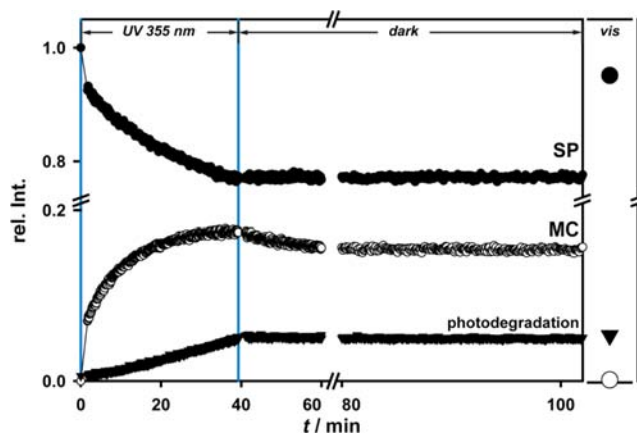


Figure 6. Relative changes in NMR signal integrals during and after irradiation of compound 4 with UV light. Peaks of the SP form (filled circles, average derived from H2, H6, H8, H17, H23; for assignment, see Supporting Information) decay during UV irradiation, whereas signals from the MC form (open circles, average derived from H6, H7, H14, H22, H23) and of photodegradation products (filled triangles) rise in intensity. Integrals are averaged over well-resolved signals for each form. The three data points on the right-hand side of the graph display the relative integrals of NMR signals after irradiation outside the NMR spectrometer with visible light ($T = 275$ K). The size of the symbols represents the measurement uncertainties calculated from the standard deviation of the respective signal integrals.

278 K. This rate is significantly enhanced upon acidification. Consistent with our data, the MC form present in the thermal equilibrium is protonated at low pH and the purple color disappears. Toward more basic pH conditions (beyond $pH^{(2)}$), the MC form undergoes a fast depopulation due to hydrolysis with the rising concentration of OH^- . It is important to note that the pH behavior shown in Figure 4 is (pseudo)reversible—going

back to neutral pH conditions—due to deprotonation of the phenolic OH group and due to a slow-down of the hydrolysis leading to a repopulation of the little amount of the purple colored MC form in the thermal equilibrium (see also Supporting Information).

A difference spectrum between an irradiated and a non-irradiated sample isolates the signals of the MC form of compound **4** (Figure 5c). The configuration of the double bond is (*E*) ($^3J(\text{H,H}) = 16.5 \text{ Hz}$). Subsequent irradiation of the NMR sample with visible light completely shifts the equilibrium back to the SP form. In contrast, the thermal back reaction occurs slowly; even after 13 h signals of the MC form can still be detected in the NMR spectrum.

For an application in a cellular environment it is important that the photoswitch is stable under those conditions and that it is not toxic. As previously noted, azobenzenes are known to be reduced for example by glutathione⁹ and spiropyran can undergo a hydrolysis reaction at physiological pH conditions which leads to decomposition.¹⁵ Therefore, we investigated the hydrolysis of compounds **2–4** in PBS buffer (pH 7.4), in TRIS buffer (pH 7.6), and in HeLa cell extracts (see Supporting Information). Under all the chosen conditions only negligible hydrolysis was found within a time range of 5 days and even after 60 days more than 50% remained intact. This is in stark contrast to the hydrolysis of Nitro-BIPS derivatives which is known to occur within hours.¹⁵

Finally, we assessed the effects of compounds **2–4** on HeLa cellular viability and saw only little effects on up to a concentration of 100 μM (Supporting Information). With the highest used concentration of 1 mM compound **2** exhibits a reduction of viability to 50%, whereas compounds **3** and **4** showed only a slightly decreased cellular viability. The little adverse effects on cellular viability of compounds **2–4** at a 100 μM concentration and for compounds **3** and **4** even at 1 mM concentration strongly indicate that these compounds can be used in cellular applications without any drawback.

In summary, following our initial study focusing on ultrashort dynamics of Py-BIPS derivatives¹⁸ we have demonstrated that these compounds are indeed a very promising new subclass of spiropyran which possesses many favorable properties for application in a biological context. Major advantages are high solubility and hydrolytic stability as well as low toxicity and most important of all the suitable photoswitching behavior. Thus, with its properties Py-BIPS and its derivatives nicely complement the few available spiropyran derivatives which are compatible with an application in water.^{20–22}

■ ASSOCIATED CONTENT

📄 Supporting Information

Synthetic procedures and (photophysical) characterization, toxicological and hydrolysis studies. This material is available free of charge via the Internet at <http://pubs.acs.org>.

■ AUTHOR INFORMATION

Corresponding Authors

*E-mail: wweilt@theochem.uni-frankfurt.de.

*E-mail: heckel@uni-frankfurt.de.

Author Contributions

||C.Ö., T.H., and S.S. contributed equally.

Notes

The authors declare no competing financial interest.

■ ACKNOWLEDGMENTS

We thank Frank Schroll and Chokri Boumrifak (Goethe-University Frankfurt, Institute for Physical and Theoretical Chemistry) for their support regarding the photochemical characterization of the spiropyran compounds and the Deutsche Forschungsgemeinschaft (DFG) through SFB 902 “Molecular Principles of RNA-based Regulation” for funding. Work at BMRZ is supported by the state of Hesse.

■ REFERENCES

- (1) Brieke, C.; Rohrbach, F.; Gottschalk, A.; Mayer, G.; Heckel, A. *Angew. Chem., Int. Ed.* **2012**, *51*, 8446.
- (2) Göstl, R.; Senf, A.; Hecht, S. *Chem. Soc. Rev.* **2014**, *43*, 1982.
- (3) Szymański, W.; Beierle, J. M.; Kistemaker, H. A. V.; Velema, W. A.; Feringa, B. L. *Chem. Rev.* **2013**, *113*, 6114.
- (4) Natali, M.; Giordani, S. *Chem. Soc. Rev.* **2012**, *41*, 4010.
- (5) Stein, M.; Middendorp, S. J.; Carta, V.; Pejo, E.; Raines, D. E.; Forman, S. A.; Sigel, E.; Trauner, D. *Angew. Chem., Int. Ed.* **2012**, *51*, 10500.
- (6) Tanaka, F.; Mochizuki, T.; Liang, X.; Asanuma, H.; Tanaka, S.; Suzuki, K.; Kitamura, S.; Nishikawa, A.; Ui-Tei, K.; Hagiya, M. *Nano Lett.* **2010**, *10*, 3560.
- (7) Nishioka, H.; Liang, X.; Kato, T.; Asanuma, H. *Angew. Chem., Int. Ed.* **2012**, *51*, 1165.
- (8) Koger, A.; Walko, M.; Meijberg, W.; Feringa, B. L. *Science* **2005**, *309*, 755.
- (9) Boulègue, C.; Löweneck, M.; Renner, C.; Moroder, L. *ChemBioChem* **2007**, *8*, 591.
- (10) Singer, M.; Nierth, A.; Jäschke, A. *Eur. J. Org. Chem.* **2013**, 2766–2013.
- (11) Andersson, J.; Li, S.; Lincoln, P.; Andréasson, J. *J. Am. Chem. Soc.* **2008**, *130*, 11836.
- (12) Jonsson, F.; Beke-Somfai, T.; Andréasson, J.; Nordén, B. *Langmuir* **2013**, *29*, 2099.
- (13) Hammarson, M.; Nilsson, J. R.; Li, S.; Beke-Somfai, T.; Andréasson, J. *J. Phys. Chem. B* **2013**, *117*, 13561.
- (14) Bletz, M.; Pfeifer-Fukumura, U.; Kolb, U.; Baumann, W. *J. Phys. Chem. A* **2002**, *106*, 2232.
- (15) Stafforst, T.; Hilvert, D. *Chem. Commun.* **2009**, 287.
- (16) Beyer, C.; Wagenknecht, H.-A. *Synlett* **2010**, 1371.
- (17) Brieke, C.; Heckel, A. *Chem.—Eur. J.* **2013**, *19*, 15726.
- (18) Kohl-Landgraf, J.; Braun, M.; Özçoban, C.; Gonçalves, D. P. N.; Heckel, A.; Wachtveitl, J. *J. Am. Chem. Soc.* **2012**, *134*, 14070.
- (19) ACD/Labs, Percepta 2012.
- (20) Tomizaki, K.; Mihara, H. *J. Am. Chem. Soc.* **2007**, *129*, 8345.
- (21) Young, D. D.; Deiters, A. *ChemBioChem* **2008**, *9*, 1225.
- (22) Hammarson, M.; Nilsson, J. R.; Li, S.; Lincoln, P.; Andréasson, J. *Chem.—Eur. J.* **2014**, *20*, 15855.